Published in final edited form as:
J Biomed Opt. 2009 ; 14(3): 030512. doi:10.1117/1.3155523.

Speckle reduction in optical coherence tomography using angular compounding by B-scan Doppler-shift encoding

Hui Wang and **Andrew. M. Rollins**
Department of Biomedical Engineering, Case Western Reserve University

Hui Wang: Hxw26@case.edu

Abstract

We propose a novel method for speckle reduction for optical coherence tomography based on angular compounding by B-scan Doppler-shift encoding (AngularCBD). By de-centering the probe beam from the pivot of a scanning mirror, the illumination angle represented by different components of the beam can be encoded in Doppler shift. Compounding multiple images reconstructed from different Doppler-shift bands, we can suppress speckle without sacrificing image acquisition speed. Speckle reduction with AngularCBD is demonstrated by imaging a phantom and tissue sample *in vitro* and *in vivo*.

Keywords

Speckle reduction; Optical Coherence Tomography; Doppler shift; Angular compounding

In optical coherence tomography (OCT) imaging, speckle arises from multiple scattering in the sample and degrades the visibility of fine structures in images. However, speckle is also the carrier of the information of tissue structure. Many efforts have been made to reduce speckle in OCT. In general, noise can be suppressed by averaging if successive acquisitions contain the same signal but uncorrelated noise. Speckle can be suppressed in this way by using frequency compounding, polarization compounding or angular compounding (1–5). Speckle reduction by angular compounding has been realized by multiple methods that involve acquiring multiple images with slightly different beam incidence angles (2, 6, 7). This has required sacrificing imaging speed or use of bulky optical components (4, 6–9). Angular compounding by path length encoding (ACPE) can suppress speckle without reducing imaging speed(2). However, ACPE requires a long imaging range in order to separate the images from different angles. So it is difficult to achieve this with spectral-domain OCT (SDOCT). Also, the necessary delay element introduce extra dispersion which could be a problem using ultra-high resolution OCT. Here, we introduce a novel and simple method to suppress speckle, angular compounding by B-scan Doppler shift encoding (AngularCBD).

A schematic of AngularCBD is shown in Fig. 1 (a), which represents a typical sample arm used in a bench top OCT. The collimated beam in the sample arm is aligned offset from the pivot of the scanning mirror, so that a Doppler shift is introduced during the course of a B-scan. This principle has been previously proposed for generating a carrier signal for en-face time-domain OCT imaging,(10) and has more recently been used to resolve the complex-conjugate ambiguity in SDOCT(11–13). Because the sample beam is incident on a range of positions on the scanning mirror before the objective lens, different incidence angles are encoded by different Doppler shifts. It has been shown that the Doppler shift is linearly proportional to the offset from the pivot of the scanning mirror(11).

To illustrate the concept, an experiment was conducted by physically blocking halves of the beam alternatively. The corresponding Doppler shifts are shown in Fig. 1 (b). A phantom made by mixing 2% intralipid and agarose gel was imaged with SDOCT at 1300 nm. The axial resolution of the system was 14 μm in air. The beam in the sample arm, with a beam diameter of about 6 mm, was focused by an achromatic lens with a focal length of 35mm to a spot of 10 μm in diameter. With a power at the sample of 10 mW, the sensitivity was measured to be 110 dB with −6 dB decay at 2 mm. The center of the beam was offset from the pivot by 4.2 mm, which introduce a Doppler shift about 8 kHz during a B-scan. All images were acquired at 40k A-scans/s. Each frame consists of 1000 A-scans across 2.5 mm on the sample, resulting in a transverse imaging pitch of 2.5 μm. The half-beams 1 and 2 were blocked alternately as illustrated in Fig. 1 (a). The Doppler-shift acquired over the course of a B-scan was calculated by Fourier transform of the data at one pixel of the photodiode array. With half-beam 1 blocked, only the signal from path 2–2 was acquired and the observed Doppler shift was concentrated in the higher frequency range, as shown in Fig. 1 (a) and (b). Similarly, the observed Doppler shift was in the lower frequency range when half-beam 2 was blocked. The gap between the 1–1 and 2–2 represents the Doppler shift from beams 1–2 and 2–1, which was lost by blocking the half beam.

The angle encoded Doppler shift can be used to reconstruct multiple OCT images representing different illumination/collection angles. We used a moving window to band-pass filter the B-scan Doppler shift spectrum. Separated images were achieved by reconstructing OCT images from the filtered Doppler shift bands, which were then summed to form the final image. Since the separated images are angle-dependent, they contain different speckle patterns. Therefore, speckle reduction can be expected by image compounding. The same phantom employed in Fig. 1 was also used to quantify the speckle contrast after speckle reduction. A moving Tukey window was used to filter the B-scan Doppler shift spectrum as shown in Fig. 1 (b) without beam blocking. Fig. 2(a) shows the five filtered B-scan Doppler shift sub-bands with the moving window. Fig. 2 (b) plots images reconstructed from the sub-bands 1, 2, 3. To quantify the correlation of the speckle patterns between different sub-band images, the cross correlation coefficients were calculated following a previously described method (3), where the exponential decay with depth was first corrected and then an area of about 200×200 μm^2 was selected for calculation. Fig. 2(c) shows the speckle cross correlation between sub-band images. The cross correlation between the neighbor images in Fig. 2 (b) is below 0.1. This confirms that each image predominantly represents independent speckle patterns resulting from different illumination/collection angles. Therefore, speckle reduction can be expected after compounding the five images. For comparison, the original image and the image after speckle reduction are shown in Fig. 3. The speckle contrast C is defined as the ratio of the standard deviation to the mean of the pixel values in the selected region. The speckle contrast of Fig 3 (a) is 0.57, which is very close to the theoretical value of 0.52 for fully developed speckle(3).. After image compounding, the speckle contrast is 0.31 measured from the same region. Thus speckle contrast has been reduced by a factor of 1.84. A reduction factor of 2.2 is expected for five independent angle related images(3). The difference can be attributed to non-uniform light power distribution between the five filtered sub-bands and residual overlap between the subbands. Significant reduction of variation caused by speckle along single A-scan is shown in Fig. 3 (c) and (d) as well as shown in the images of Fig. 3 (a) and (b).

While significant speckle reduction is achieved, implementation of AngularCBD requires a compromise between speckle reduction and lateral resolution. Because only part of the beam is used for each sub-image, the effective imaging N.A is reduced by the band-pass filter. To measure the transverse resolution reduction factor, a USAF target with multiple parallel bars covered by a phantom with a thickness of 600 μm was imaged, and the slope of the edges of

the bars across a B-scan was measured. The lateral resolution was found to be reduced by a factor about 1.84. A simple blurring function can also be expected to reduce speckle contract. Therefore, in order to demonstrate that the AngularCBD method is not simply equivalent to a lateral blur, a rolling average of seven neighboring A-scans was computed on the original image, and the result is shown in Figure 3 (c). As a result, the lateral resolution was reduced by a factor about 1.72, closely matching the resolution reduction resulting from the AngularCBD processing. The speckle contrast was reduced by the blur to 0.49, which represents a factor of 1.16 reduction, much less than the reduction factor achieved by AngularCBD. For achieving similar effect of speckle reduction as AngularCBD, twenty one neighboring A-scans were required for averaging. However, the lateral resolution was significantly reduced.

We demonstrated the technique by imaging biological tissue samples *in vivo and in vitro*. Speckle reduction is apparent and fine structures are visualized with better contrast after AngularCBD, as shown in Fig. 4 (b) compared to the original image (a) by imaging a living Quail embryo *in vivo*. Figures 4 (c) and (d) show images of a porcine esophagus *in vitro* before and after AngularCBD. The layered structures are better defined after AngularCBD.

Further speckle reduction is possible by choosing a smaller filtering window to increase the number of angle–related sub-band images. However, the lateral resolution will be decreased further. In this study, a Tukey window was chosen here although other kinds of windows are feasible. Just increasing the number of sub-band images with a fixed width window does not improve the speckle reduction further due to increased sub-band overlap. AngularCBD method is very flexible, because all processing is carried out after image acquisition. The width and the number of the windows can be chosen based on the sample and desired speckle reduction factor. As other B-scan Doppler methods, transverse sampling must be sufficient to sample the full speckle pattern.

In practical implementation, the method is straightforward to optimize, based on the limitation of the size of the scanning mirror. In order for the entirety of the B-scan Doppler spectrum to be shifted to one side of dc, the entirety of the beam should be offset to one side of the mirror pivot. It will be good to choose a larger beam to compensate the loss of the lateral resolution after ABCD.

If there is flow or motion in the tissue being imaged, an additional Doppler shift will be imposed on the sample beam, which will up-shift or down-shift the B-scan Doppler frequency at that location. Thus, the flow signal will be translated to different locations in the B-scan Doppler spectrum. This effect has been used for Doppler OCT flow imaging(14), but should not affect the AngularCBD method as long as the range of the B-scan Doppler spectrum analyzed encompasses the shifted signal components. Therefore, AngularCBD can be used simultaneously with deconjugation of the mirror images in SDOCT and flow tracking (11–14).

In conclusion, we have introduced a novel method, AngularCBD, to reduce speckle in OCT images. We demonstrated speckle reduction by a factor of 1.84 by incoherently adding five Doppler shift angle encoded images. AngularCBD is compatible with most typical OCT scanners making use of tilting mirrors. Important features of ANGULAR-BD are that it does not interfere with the frame rate nor introduce any optical nor mechanical components nor extra dispersion. The only needed modification to a conventional scanner is to de-center the beam from the pivot of the scanning mirror, which is typically readily realizable.

References

1. Schmitt JM, Xiang SH, Yung KM. Speckle in Optical Coherence Tomography. Journal of Biomedical Optics. 1999; 4(1):95–105. [PubMed: 23015175]
2. Iftimia N, Bouma BE, Tearney GJ. Speckle reduction in optical coherence tomography by “path length encoded” angular compounding. Journal of Biomedical Optics. 2003; 8(2):260–263. [PubMed: 12683852]
3. Pircher M, Gotzinger E, Leitgeb R, Fercher AF, Hitzenberger CK. Speckle reduction in optical coherence tomography by frequency compounding. Journal of Biomedical Optics. 2003; 8(3):565–569. [PubMed: 12880365]
4. Kim J, Miller DT, Kim E, Oh S, Oh J, Milner TE. Optical coherence tomography speckle reduction by a partially spatially coherent source. Journal of Biomedical Optics. 2005; 10(6):064034–064039. [PubMed: 16409099]
5. Desjardins AE, Vakoc BJ, Tearney GJ, Bouma BE. Speckle Reduction in OCT using Massively-Parallel Detection and Frequency-Domain Ranging. Opt Express. 2006; 14(11):4736–4745. [PubMed: 19516630]
6. Schmitt JM. Array detection for speckle reduction in optical coherence microscopy. Physics in Medicine and Biology. 1997; 7:1427. [PubMed: 9253050]
7. Desjardins AE, Vakoc BJ, Oh WY, Motaghiannezam SM, Tearney GJ, Bouma BE. Angle-resolved Optical Coherence Tomography with sequential angular selectivity for speckle reduction. Opt Express. 2007; 15(10):6200–6209. [PubMed: 19546925]
8. Bashkansky M, Reintjes J. Statistics and reduction of speckle in optical coherence tomography. Opt Lett. 2000; 25(8):545–547. [PubMed: 18064106]
9. Popescu DP, Hewko MD, Sowa MG. Speckle noise attenuation in optical coherence tomography by compounding images acquired at different positions of the sample. Optics Communications. 2007; 269(1):247–251.
10. Podoleanu AG, Dobre GM, Jackson DA. En-face coherence imaging using galvanometer scanner modulation. Opt Lett. 1998; 23(3):147–149. [PubMed: 18084441]
11. An L, Wang RK. Use of a scanner to modulate spatial interferograms for in vivo full-range Fourier-domain optical coherence tomography. Opt Lett. 2007; 32(23):3423–3425. [PubMed: 18059954]
12. Baumann B, Pircher M, Gʊzinger E, Hitzenberger CK. Full range complex spectral domain optical coherence tomography without additional phase shifters. Opt Express. 2007; 15(20):13375–13387. [PubMed: 19550607]
13. Leitgeb RA, Michaely R, Lasser T, Sekhar SC. Complex ambiguity-free Fourier domain optical coherence tomography through transverse scanning. Opt Lett. 2007; 32(23):3453–3455. [PubMed: 18059964]
14. Wang RK, Jacques SL, Ma Z, Hurst S, Hanson SR, Gruber A. Three dimensional optical angiography. Opt Express. 2007; 15(7):4083–4097. [PubMed: 19532651]

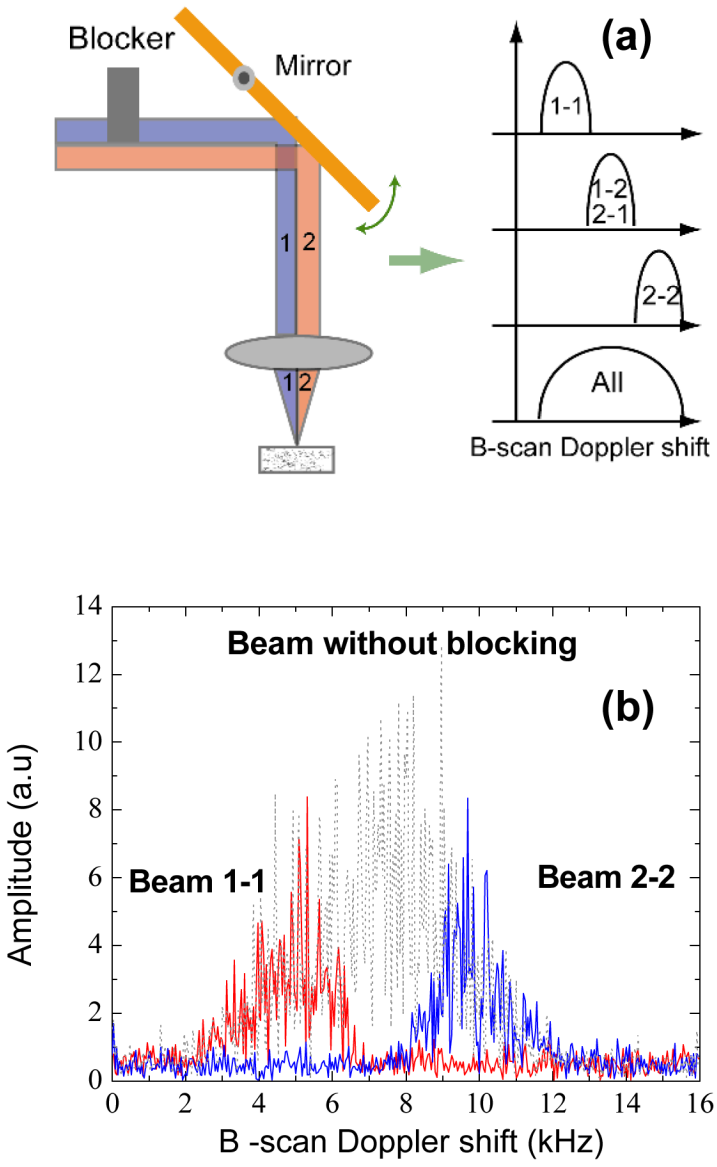

Figure 1.
(a) The schematic of the scanner used for AngularCBD and angle encoded Doppler shift spectrum by physically blocking part of the beam. (b) Measured angle encoded Doppler shift spectrums, which are illustrated in (a). The spectrum was measured with a uniform phantom described in the context.

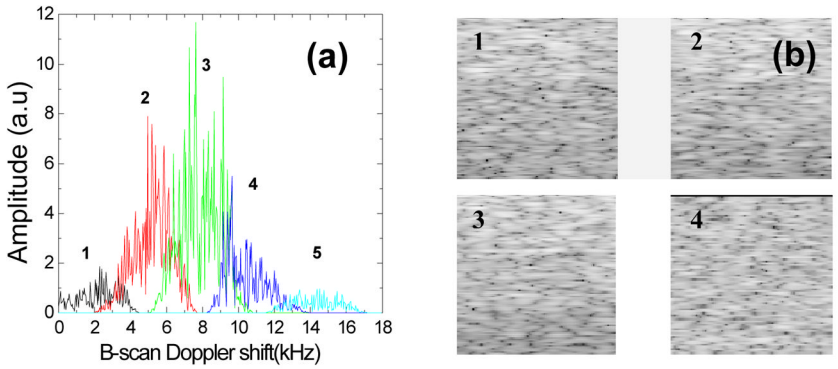

Figure 2.

(a) Five B-scan Doppler shift sub-bands filtered with a moving Tukey window with a width of 150 points. (b) The corresponding images of sub-bands 1 2 3 4 (50×50 μm^2) and (c) cross correlation of speckle between the five images. The image pixel values have been normalized for display and are shown in logarithmic scale.

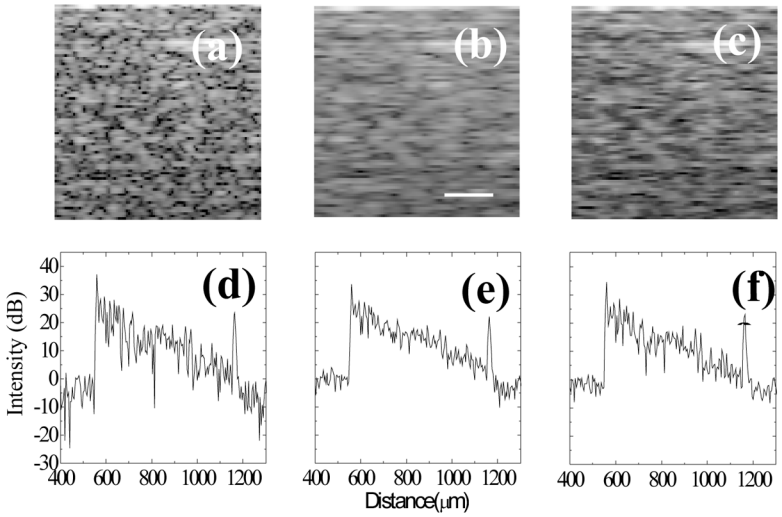

Figure 3.

A segment of the original image without speckle reduction (a), the image after AngularCBD speckle reduction (b), and a image after a 7-A-scan rolling average (c). (d–f) Single B-scans of the entire depth of phantom images. Images are shown in logarithmic scale. Scale bar: 50 μm

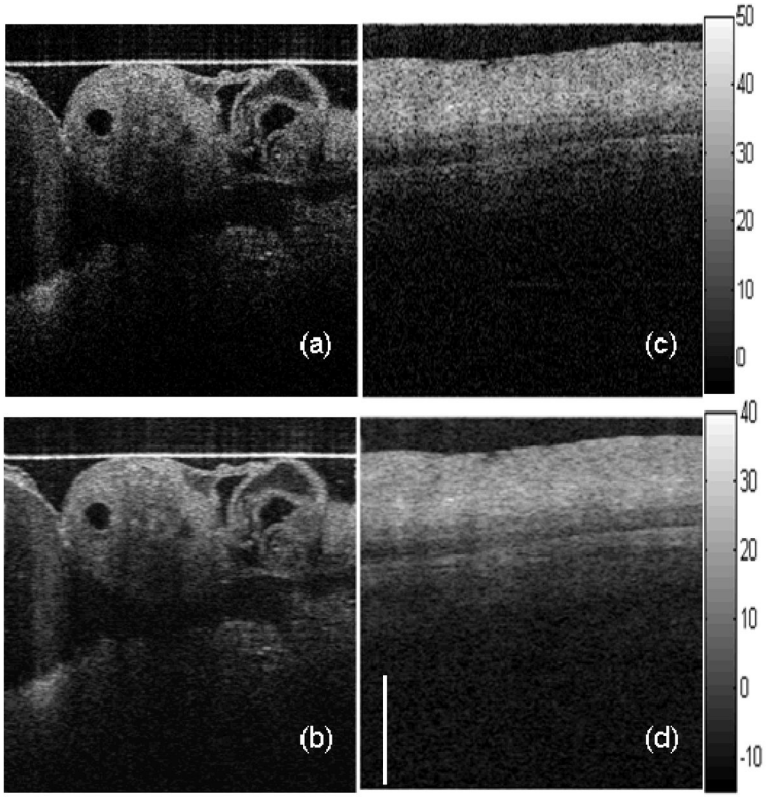

Figure 4.
In vivo image of quail embryo before (a) and after AngularCBD (b); *In vitro* porcine esophagus before (c) and after AngularCBD (d). Contrast of fine structures and layers are clearly enhanced after speckle reduction. Images are shown in logarithmic scale. Scale bar: 1 mm